CO2 laser surface engineering of polyethylene terephthalate (PET) for enhanced meat exudate conditioning film formation and bacterial response

Lawrence, J. & Waugh, D.

Original citation & hyperlink:
Lawrence, J & Waugh, D 2017, 'CO2 laser surface engineering of polyethylene terephthalate (PET) for enhanced meat exudate conditioning film formation and bacterial response' Lasers in Engineering, vol. 38, no. 1-2, pp. 37-56.

ISSN 0898-1507
ESSN 1029-029X

Publisher: Old City Publishing

CO_2 Laser Surface Engineering of Polyethylene Terephthalate (PET) for Enhanced Meat Exudate Conditioning Film Formation and Bacterial Response

J. LAWRENCE* AND D.G. WAUGH

School of Mechanical, Aerospace and Automotive Engineering, Faculty of Engineering, Environment and Computing, Coventry University, Gulson Road, Coventry, CV1 2JH, UK

*Corresponding author: E-mail: jonathan.lawrence@coventry.ac.uk, jl-laserengineering@hotmail.com

ABSTRACT

The attachment of bacteria to a surface is initiated by the absorption of molecules to the surface of a substratum forming what is known as a conditioning film. The nature of conditioning films may be quite different depending on the type of environment the surface is exposed to. To date, limited studies on *E. coli* biofilms have been performed, which mimic the conditions encountered in the food processing and packaging environment, and so any research into this area is timely. The benefits of CO_2 laser surface engineering on the physical properties of polyethylene terephthalate (PET) films, and the subsequent effects on conditioning film formation and bacterial response are presented. The influence of interfacial wetting on initial conditioning of the laser surface engineered PET film was analysed using contact angle measurements. Thereafter the equation of state approach was used to explain the relationship between laser engineered surface characteristics, wettability characteristics and conditioning film formation. Through this work it is clear that laser surface engineering significantly influenced the initial interfacial wettability characteristics of the PET, creating hydrophobic surfaces. Generally, the conditioning film was responsible for reducing the overall hydrophobic characteristics of the CO_2 laser surface engineered samples. Bacterial adhesion analysis revealed a bacterial response to the CO_2 laser engineered patterns (track and hatch) resulted in modulation of the distribution

and morphology of the attached cells. This is significant as it presents the viability of laser surface engineering for creating anti-bacterial and bacteria-reactive surfaces at scale, highlighting the potential for deployment of laser surface engineering in the food manufacturing industry.

Keywords: CO_2 laser, surface engineering, conditioning film, wettability, biofilm, food packaging

1 INTRODUCTION

The effective colonization of bacteria to surfaces and subsequent formation of biofilms in nearly all habitats where life can exist occurs as a result of the proficiency of bacteria to adapt to not only their extracellular surroundings but also environmental conditions [1-9].

In the food industry biofilms have been found to persist on food processing equipment, then detach and contaminate other surfaces, including those in direct contact with food [9-12]. Such contamination can lead to food spoilage problems or potential public health concerns [9]. The build-up of leaked foodstuffs or runoff of meat exudate contain a complex blend of proteins, carbohydrates, lipids, and sugars [10], providing nutrition rich conditioning layers ideal for bacteria to thrive and survive [10, 13, 14]. Bonding between bacteria and conditioning film is mostly mediated by specific extracellular proteinaceous components, known as adhesins, and complimentary receptors on the surface; that is, proteins [15]. The physical properties of a conditioning film including its composition, packing and density are largely dependent on the physical and chemical nature of the underlying substratum [15].

Strategies to prevent and combat bacterial attachment and subsequent biofilm formation include surfaces with chemical modification with antibacterial agents (antibiotics, antimicrobial peptides, detergents, metals and alkyl chains) [16]. Although these surfaces are known to be effective, they are subject to many limitations; for example, if the modified surface has been produced using a chemical antibacterial mechanism, the pharmacodynamics and kinetics need to be thoroughly evaluated especially as the functionalised surface may undergo further reactions which may adversely affect their bactericidal properties [17, 18]. For bioactive surfaces, it is possible for bacteria to develop resistance against the active agent and it can also take a long

time for the release of antibacterial agents from the surface. With bioactive surfaces, it is also possible that the durability of target substrate may not be sufficient to maintain long-term antibacterial activity. Alternative strategies includes the physical modification of surface topography, which is receiving far greater consideration due to these complexities [19, 20]. Laser surface engineering is a subject of considerable interest due to its ability to produce enhanced components with idealized surfaces and bulk properties [21]. Laser engineered surfaces which influence the formation and/or composition of the initial conditioning film could provide insight in to influencing and/or preventing the early stages of biofilm formation.

In this study, surface characteristics and contact angle measurements were investigated in order to explain the relationship between laser-modified surface parameters, wettability characteristics and conditioning film formation, the precursor to bacterial attachment, on laser surface engineered polyethylene terephthalate (PET).

2 EXPERIMENTAL DETAILS

2.1 Material specification and laser surface engineering procedure

PET films (Goodfellow, Ltd.), biaxially oriented and of a 0.25 mm thickness were used for the experimentation. Prior to etching, the films were cleaned in acetone and then in ethanol for three minutes each at room temperature then dried in a sample drier for a minimum of an hour.

Post cleaning the PET films were etched using a 60 W CO_2 laser system (Firestar; Synrad, Inc.) including a galvanometric scanning head. This CO_2 laser emitted a Gaussian beam at 10.60 μm in the continuous wave (CW) mode. In order to create the desired pattern upon the PET film surface Synrad Winmark Pro software (Synrad, Inc.) was used to scan the laser beam within a square working field of 110 × 110 mm^2. Samples were cut into 10 × 15 cm^2 billets which were then secured down and positioned at the focal point which was 190 mm away from the surface of the sample to the focussing lens on the galvanometric head. All samples were treated in ambient air and an extraction system was used to remove any fumes produced during the laser processing. Constant laser parameters were used for all patterns produced. The power was set to 10.0% (6 W), the transverse scanning speed was set to 400 mm/s and the spot size was maintained at 95 μm. Two different track and two different hatch patterns were produced: tracks with 350.00 μm and 400.00 μm spacing between each line were used to create the different CO_2 laser surface

engineered patterns. These track samples were labelled CO2SP_04 and CO2SP_05 and the hatch samples were labelled CO2HA_04 and CO2HA_05, for 350.00 and 400.00 μm spacings, respectively, for both patterns. It should be noted here that the dimensions stated for the laser engineered samples are those of the CO_2 laser scanning dimensions and not of the resulting laser engineered patterns.

2.2 Morphology, microstructure, phase and topographical analysis techniques

Before and after CO_2 laser surface engineering the PET films were analysed using an optical microscope (DM500; Leica Microsystems, GmbH) to determine morphology and also a scanning electron microscope (SEM) (TM3030 Plus; Hitachi Corporation) to determine the morphological and microstructural characteristics.

To ascertain phase characteristics of the as-received and CO_2 laser engineered billets X-ray photoelectron spectroscopy (XPS) data was acquired. This was done using a bespoke ultra-high vacuum system fitted with a 150 mm mean radius hemispherical analyser with a 9-channeltron detection (Phoibos; Specs GmbH). XPS spectra were acquired using a non-monochromated Al Kα X-ray source at 1486.6 eV. Survey spectra were acquired over the binding energy range 1100 to 0 eV using a pass energy of 50 eV and high resolution scans were made over the C 1s and O 1s lines using a pass energy of 15 eV. In each case the analysis was an area average over a region approximately 2 mm in diameter on the sample surface. The energy scale of the instrument is calibrated according to ISO standard 15472, and the intensity scale is calibrated using an in-house method traceable to the UK National Physical Laboratory [22]. Data were quantified using Scofield cross sections corrected for the energy dependencies of the electron attenuation lengths and the instrument transmission. Data interpretation was carried out using CasaXPS software v2.3.16.

The surface topography of the as-received and CO_2 laser engineered billets was analysed using a confocal chromatic imager (CCI) profilometer (Micromersure2, STIL SA.). Sample sizes of 0.5 × 0.5 mm^2 were examined for each of the billets analysed. Three CO_2 laser surface engineered and three as-received control billets were analysed. Modified samples were ultrasonically cleaned in acetone, ethanol then dH_2O for three minutes each at room temperature before measurements were taken. The results were analysed using SurfaceMaps software (STIL SA.) and were expressed as R_a (the arithmetic mean of the departures of the roughness profile

from the mean line) and S_a (the surface roughness calculated over an area) [36]. Data for R_t (maximum height of profile) and R_{sk} (skewness; symmetry of the profile about the mean) surface parameters were included in order to provide more information on the topographical features of the surfaces.

2.3 Wettability characteristics analysis methodology

Wettability was quantified through contact angle measurements obtained using a goniometer (OCA20; DataPhysics, GmbH) using the needle-in advancing method. Prior to contact angle measurements being taken the billets were ultrasonically cleaned in acetone, ethanol and finally dH_2O for three minutes each at room temperature. The dH_2O step was included here to remove any residue left on the PET surface resulting from the acetone and ethanol cleaning stages. To ensure that the sample surfaces were dry, the billets were placed in a specimen dryer (SS; LEEC, Ltd.) for 30 minutes before contact angle measurements were taken. For preconditioned samples the contact angle measurements were taken as described above; however, the samples were not cleaned before analysis. At the prescribed time points each sample was removed and rinsed in dH_20 to remove any excess exudate then allowed to air dry before analysis.

2.4 Conditioning film growth conditions

Exudate from beef was obtained by thawing frozen cuts of beef purchased from a local superstore. In accordance with an adapted method from Midelet and Carpentier [10], 500 g of the meat was cut into 1 × 1 square inch pieces and placed in two plastic food bags. The meat was then put in a large sealed plastic bag and weighed down and frozen at -20°C. It took 48 hours at 5°C to thaw the meat, which produced 25 ml of exudate. Excess exudate was kept at 20°C and used within the following four months. After the tubes were thawed and the meat exudate was centrifuged at 11000 g for 15 minutes. The supernatant was then filtered through a 0.22 µm pore size filter with a 1.60 and 0.45 µm pre-filter (Whatmann; Sigma Aldrich, Inc.). Samples were preconditioned with the meat exudate by adding 1 ml of the filtered exudate to 24-well plates. Substrates with diameters of 15 mm from all patterned and as-received PET samples were aseptically added to the plates, which were then incubated at 37^{o}C.

2.5 Bacterial attachment and biofilm development

E. coli wild type ATCC strain 25922 was purchased as a 'cultiloop' (Oxoid, Ltd.) and used in this work. Cultiloops were stored at 5^{o}C until they were required. For the analysis of *E. coli* attachment under static conditions overnight cultures of each of the *E. coli* strains were diluted to an O.D. reading of 0.01 [23] before 1 ml of culture was added to 24-well plates. Substrates with diameters of 15 mm from all CO_2 laser engineered and as-received PET samples were aseptically added to the plates, which were then incubated at 37^{o}C. In order to evaluate biofilm growth all samples were aseptically removed after 24 hours. Samples were then rinsed twice with sterile (phosphate-buffered saline (PBS) solution to remove any planktonic bacteria. Preconditioned samples were incubated with the meat exudate for an hour at 37^{o}C, after which the exudate was carefully pipetted out of each well. 1 ml of PBS solution was then used to rinse each well twice before the diluted bacteria.

Samples were then prepared for SEM examination by washing with 0.1M sodium cacodylate and fixing in 2.5% glutaraldehyde in 0.1M sodium cacodylate for 30 minutes. Fixed specimens were then washed twice in dH_2O, dehydrated for 10 minutes at each stage of an ascending ethanol series (50.0 to 100.0%) and left to air dry for 30 minutes. Each sample was coated in a thin Au layer before being analysed under the SEM at a working distance of 10 mm. 10 random locations were visualized.

In order to enumerate the quantity of bacteria attached to the different billets, each sample was placed separately into a sterile 25 ml plastic universal tube containing 5ml PBS. The universals were then vortexed vigorously [24], log diluted using PBS, and spread plated on tryptic soy agar plates. Plates were then incubated at 37^{o}C for 24 hours before analysing.

2.6 Statistics methods

Statistical analysis was performed by two-way analysis of variance combined with Tukey's Post Hoc analysis with $p \geq 0.05$ considered significant. All data has been analysed using SPSS statistics 22.0 (IBM) and graphical representation of results were produced using SigmaPlot 13.0 (Systat Software, Inc.).

3 RESULTS AND DISCUSSION

3.1 Topographical observations following CO_2 laser surface engineering

Optical and SEM micrographs of the laser engineered surface patterns are shown in Figure 1. The optical micrographs of the samples demonstrate the change to the surface of the CO_2 laser engineered PET samples relative to the as-received control sample. Previous results have shown lasers to be effective tools for engineering specific and unique topographical features on a number of polymeric materials [25-27]. The patterns of the PET film surfaces engineered by the CO_2 laser beam interaction depend upon both the optical system parameters of the CO_2 laser experimental configuration and the material properties of the polymer [28]. The laser parameters determine the incident laser power, spot size, depth of field and divergence of the laser beam, while the thermophysical properties of the polymer determine how the polymer reacts to the beam. The resulting profile of the CO_2 laser engineered patterns and the heat affected zone (HAZ) are a result of the combination of these factors [28].

From the SEM micrographs shown in Figure 1 it can be seen that as a direct result of the interaction of the CO_2 laser beam with the PET film surfaces, features were created *via* controlled melting, as depicted by the craters formed from bubbles, and subsequent resolidification which has formed the different track patterns. This complicated structure is likely associated with the thermally induced stress release in the biaxially oriented film caused by the laser beam interaction with the PET film [29].

In comparison to the track patterns, both hatch patterns have resulted in wider tracks being formed along the ordinate direction of the pattern. This is because the CO_2 laser beam actually processes the PET surface twice, with the CO_2 laser beam passing over the initial track to create the hatch, causing the PET surface to remelting and resolidify, naturally creating larger surface features. The remelting and resolidification of the material on the hatch pattern has also resulted in some of the patterning becoming changed. Where the CO_2 laser beam has passed over the underlying track, the sides have been remelted and part of the track has subsequently filled in. Even so, the overall hatch and track patterns appear clean and well structured. It is worth noting that no discernible HAZ was observed under optical microscopic analysis (see Figure 1) and, therefore, the areas between the tracks were considered as as-received material.

The value of the R_a parameter was found to have increased considerably from 0.06 ±0.01 µm for the as-received control sample (CO2SP_AR) up to 8.64 ±0.10 µm for CO2SP_04 and

6.22 ± 0.79 µm for CO2SP_05 (see Table 1). Similarly, the value of the S_a surface roughness parameter experienced a marked increase from 0.22 ±0.13 µm for the as-received control sample (CO2SP_AR) up to 22.80 ±4.43 µm for CO2SP_04 and 10.47 ±0.12 µm for CO2SP_05. The increase in surface roughness between CO2SP_AR and both CO2SP_04 and CO2SP_05 was found to be statistically significant with a mean difference of 8.58 µm, $p<0.01$, and 6.62 µm, $p<0.01$, for R_a; and 22.58 µm, $p<0.01$, and 10.24 µm, $p=0.01$, respectively for S_a (see Table 1).

For samples labelled CO2HA_ both the R_a and S_a surface parameters were found to have considerably increased compared to the as-received sample (CO2SP_AR), as can be seen in Table 2. This discernible increase in surface roughness between the as-received sample and both hatch patterned samples was found to be statistically significant, $p<0.05$. Interestingly, as well as an overall increase in surface roughness, the surface roughness for CO2SP_04 and CO2HA_04 was found to significantly increase compared to that of wider spaced track and hatch patterns (sample CO2SP_05 and sample CO2SP_05), $p<0.05$, for both R_a and S_a. This is due to a larger surface area of the CO2SP_ 04 and CO2HA_04 samples being processing by the CO_2 laser beam which, in turn, created a markedly rougher surface.

The statistical significances between the as-received PET films and the CO_2 laser etched is unsurprising as the CO_2 laser modification produced well defined topographical features, as is apparent from the change in R_t (total height of the profile). Both hatch patterns achieved the peak/valley distances measuring 107 ±2.7^o for CO2HA_04 and 116 ±4.4^o for CO2HA_05, compare to the peak/valley distances of the single track patterned samples or the as-received sample. As discussed above, this difference is explained by the second pass of the CO_2 laser beam over the PET sample surface on the hatch pattern billets, which was 90^o to the first pass resulting in double the amount of laser surface interaction where the two tracks passed. This can also be seen in the optical and SEM images given in Figure 1.

3.2 Chemical and phase observations following CO_2 laser surface engineering

XPS data show little change in surface chemistry of the PET surfaces after laser treatment, with small differences in the levels of trace contaminants (see Table 2). This demonstrates that the CO_2 laser surface engineering technique employed is capable of generating surface features without significantly modifying the chemical composition of the layer. This is important as it demonstrates that the changes to the surface energy and wettability characteristics of the PET are

most likely due to the surface morphology changes, rather than a modification of the chemical structure of the polymer that would change its innate properties. Such a finding is in accordance with previous work using various lasers to modify the wettability characterizes of polymethyl methacrylate (PMMA) [30, 31] and polyethylene (PE) [32], where the influence of laser-induced topographical changes were found to outweigh any laser-induced chemical or phase changes.

3.3 Effect of CO_2 laser modified surface roughness and topographical features on *E. coli* adhesion

E. coli ATCC 25922 was chosen as a surrogate biofilm strain based on its comparable biofilm forming capabilities to that of *E. coli* 0157:H7, a food borne pathogenic strain of *E. coli*. Figure 2 shows the influence the CO_2 laser engineered changes in surface roughness (S_a) had on bacterial adhesion to preconditioned and unconditioned samples after six hours incubation. Figure 2 shows that on the track patterned samples (CO2SP_04 and CO2SP_05) as the surface roughness increased *via* CO_2 laser surface engineering, the amount of bacterial cells adhering to the surfaces increased. From Figure 2 it can be seen that this was not the case for the hatch patterned samples (CO2HA_04 and CO2HA_05). Hsu *et al* [33] and Valle *et al* [24] have found that bacteria selectively adhere to areas on a surface that provide some form of protection or increased surface area through microtopographical features and consideration of the results for sample set CO2HA_04 and sample set CO2HA_05 concur. Sample set CO2HA_04 had a significantly higher surface roughness compared to sample set CO2HA_05 and so one would expect this sample set to have a greater number of bacteria adhere to the surface, regardless of preconditioning. This was not the case and based on the findings of Hsu *et al* [33] and Valle *et al* [24], as well as Figure 3, it would seem reasonable to assert that the microtopographical features present on the CO_2 laser engineered hatch patterns were unable to give adequate protection for the bacteria to adhere successfully. significant as it presents the viability of laser surface engineering for creating anti-bacterial and bacteria-reactive surfaces at scale, highlighting the potential for deployment of laser surface engineering in the food manufacturing industry.

3.4 Effects of CO_2 laser modified wettability characteristics on conditioning film formation and bacterial attachment

Depending upon the laser used and the material treated, surface geometrical changes can play a role in influencing the wetting of solid surfaces [34-37]. The findings given in Table 3 would support the literature as it is clear that the wetting of the PET surfaces displayed a sensitivity to the surface modifications resulting from interaction with the CO_2 laser beam. One can see from Table 3 that the CO_2 laser surface engineering was highly effective in increasing the surface hydrophobicity of the PET surfaces (p<0.05). For the track patterns the CO_2 laser surface engineering brought about an increase in the contact angles from 77.77±2.23º to 137.41 ±2.30, 143.20 ±2.85, 114.23 ±4.42 and 116.19 ±5.48; for samples CO2SP_04, CO2SP_05, CO2HA_04 and CO2HA_05, respectively. These changes in contact angle are considerable, so much so that the PET surface has been changed from hydrophilic to almost superhydrophobic (>150º) after CO_2 laser surface engineering. It would appear from the literature [25] that the CO_2 laser engineered PET surfaces with contact angles >100º have a propensity for acting as repellents towards bacteria adhesion and the subsequent prevention of biofilm formation. Since all of the PET surfaces with CO_2 laser engineered track patterns were almost superhydrophobic, then it would be reasonable to suggest that these CO_2 laser engineered surfaces would be harder for microbes to colonize in comparison to the as-received PET film surfaces (see Table 3); however, this was not the case and so the effects of conditioning film formation must be considered.

Figure 5 shows the attachment of bacteria to the as-received samples and CO_2 laser engineered samples in terms of the contact angle measurement after the surfaces have been preconditioned with the meat exudate. The contact angle measurements show wettability properties significantly decreased for all samples once they have been preconditioned with the meat exudate (p<0.05). Interestingly, the track and hatch patterns with the closer spatial features resulted in increased wetting after being incubated with the extracted meat exudate for one hour before measurement. It is possible here that due to the larger surface features created by the CO_2 laser surface engineering, there was a larger surface area available for the protein in the conditioning film. This, in turn, subsequently increased the effective surface area for proteins to adsorb onto, resulting in the conditioning film forming quicker when compared to the track patterned samples.

The differences in the wettability characteristics changes between the different CO_2 laser engineered patterns can be explained by the nonhomogeneous layer of proteins and macromolecules that adsorb from the meat exudate on to the surface which has previously been shown to influence by different surface features [38]. No correlation was found between samples incubated in absence of media or deionized water and changes in the wettability characteristics.
The wetting phenomena has been widely studied both theoretically and experimentally in connection with the physics of surfaces and interfaces [39-42] and it has been suggested that water contact angle measurements could be used as an indicator of microbial colonisation on a surface [43]. It has been found that intermediate contact angles of 30 and 100^o do not possess features that are described as 'easy clean', meaning that the removal of bacterial and other contaminants is particularly hard, and the raised features provide platforms that are easier for microbes to adhere to, and subsequently form a biofilm [17]. Supporting the hypothesis that intermediate contact angles between 30 and 100^o are more likely to be colonized [17].

The conditioning film has been found to influence substratum surface properties including surface charge, wettability and surface free energy, which have been shown to be factors influencing the initial attachment of bacteria and subsequent biofilm formation [44, 45]. The surface energy of a solid surface provides a direct measurement of the intermolecular or interfacial attractive forces. The influence of surface energy of the CO_2 laser engineered surfaces on bacterial adhesion has had conflicting reports highlighting the complex nature of the interaction of difference bacterial species with surfaces with different ranging surface energies [46-48]. Liu *et al.* [48] concluded that bacterial adhesion may decrease or increase with increasing surface energy of substrates, depending on the physical and chemical properties of the bacteria, substrates and aqueous environment. In the case of the work presented herein the increase in surface energy, due to the formation of the conditioning film, did not result in the increase in bacterial attachment rather a decrease of bacterial attachment. This is likely to be due to the conditioning film masking the surface properties or even forming different functional groups on the substrate surface making it harder for bacteria to adhere [49].

4 CONCLUSIONS

It has been shown that a CO_2 laser can be implemented for surface engineering to induce well defined features and patterns upon the surface of the PET. The engineered surface resulted in a significantly increased hydrophobic surface, however once preconditioned with a conditioning film, the hydrophilic nature of the surface was significantly increased. It can be concluded from the work presented here, that the formation of the protenious film and bacterial adhesion are heavily influenced by the topographical features of the substratum. Also of all the key influences investigated, the formation of the conditioning film from the meat exudate had a stronger influence on the wettability characteristics than that of the topographical features. The meat exudate conditioning film is responsible for reducing the hydrophobic characteristics of the CO_2 laser surface engineered PET films. Although overall the bacterial attachment was not reduced in this study, the ability to used CO_2 laser to create patterns to influence the distribution and colonisation of bacteria could provide a potential method for manipulating bacterial attachment of *E. coli*.

REFERENCES

[1] Donlan R.M. Biofilms: Microbial life on surfaces. *Emergerging Infectious Diseases* **8**(9) (2002), 881-890.

[2] Reysenbach A.L. and Cady S.L. Microbiology of ancient and modern hydrothermal systems. *Trends in Microbiology* **9**(2) (2001), 79-86.

[3] Stoodley P., Sauer K., Davies and D.G. Costerton J.W. Biofilms as complex differentiated communities. *Annual Review of Microbiology* **56** (2002), 187-209.

[4] Hall-Stoodley L., Costerton J.W. and Stoodley P. Bacterial biofilms: From the natural environment to infectious diseases. *Nature Reviews. Microbiology* **2**(2) (2004), 95-108.

[5] Lewis K. Persister cells, dormancy and infectious disease. *Nature Reviews. Microbiology* **5**(1) (2007), 48-56.

[6] Bryers J.D. Medical biofilms. *Biotechnology and Bioengineering* **100**(1) (2008), 1-18.

[7] Gubner R. and Beech I.B. The effect of extracellular polymeric substances on the attachment of Pseudomonas NCIMB 2021 to AISI 304 and 316 stainless steel. *Biofouling* **15**(1-3) (2000), 25-36.

[8] Scheuerman T.R., Camper A.K. and Hamilton M.A. Effects of substratum topography on bacterial adhesion. *Journal of Colloid and Interface Science* **208**(1) (1998), 23-33.

[9] Robitaille G., Choiniere S., Ells T., Deschenes L. and Mafu A.A. Attachment of Listeria innocua to polystyrene: Effects of ionic strength and conditioning films from culture media and milk proteins. *Journal of Food Protection* **77**(3) (2014), 427-434.

[10] Midelet G. and Carpentier B. Transfer of microorganisms, including Listeria monocytogenes, from various materials to beef. *Applied and Environmental Microbiology* **68**(8) (2002), 4015-4024.

[11] Marchand S., de Block J., de Jonghe V., Coorevits A., Heyndrickx M. and Herman L. Biofilm formation in milk production and processing environments: Influence on milk quality and safety. *Comprehensive Reviews in Food Science and Food Safety* **11**(2) (2012), 133-147.

[12] Flint S.H., Bremer P.J. and Brooks J.D. Biofilms in dairy manufacturing plant, current concerns and methods of control. *Biofouling* **11**(1) (1997), 81-97.

[13] Siboni N., Lido, M., Kramarsky-Winte, E. and Kushmaro A. Conditioning film and initial biofilm formation on ceramics tiles in the marine environment. *FEMS Microbiology Letters* **274**(1) (2007), 24-29.

[14] Beveridge T.J., Makin S.A., Kadurugamuwa J.L. and Li Z. Interactions between biofilms and the environment. *FEMS Microbiology Reviews* **20**(3-4) (1997), 291-303.

[15] Teughels W., Assche N.V., Sliepen I. and Quirynen M. Effect of material characteristics and/or surface topography on biofilm development. *Clinical Oral Implants Research* **17** (2006), 68-81.

[16] Campoccia D., Montanaro L. and Arciola C.R. A review of the biomaterials technologies for infection-resistant surfaces. *Biomaterials* **34**(34) (2013), 8533-8554.

[17] Page K., Wilson M. and Parkin I.P. Antimicrobial surfaces and their potential in reducing the role of the inanimate environment in the incidence of hospital-acquired infections. *Journal of Materials Chemistry* **19** (2009), 3819-3831.

[18] Waugh D.G., Toccaceli C., Gillett A.R., Ng C.H., Hodgson S.D. and Lawrence J. Surface treatments to modulate bioadhesion: A critical review. *Reviews of Adhesion and Adhesives* **4**(1) (2016), 69-103.

[19] Ivanova E.P., Hasan J., Webb H.K., Gervinskas G., Juodkazis S., Truong V.K., Wu A.H., Lamb R.N., Baulin V.A., Watson G.S., Watson J.A., Mainwaring D.E. and Crawford R.J. Bactericidal activity of black silicon. *Nature Communications* 4 (2013), 2838.

[20] Feng G., Cheng Y., Wang S.Y., Hsu L.C., Feliz Y., Borca-Tasciuc D.A., Worobo R.W. and Moraru C.I. Alumina surfaces with nanoscale topography reduce attachment and biofilm formation by Escherichia coli and Listeria spp. *Biofouling* **30**(10) (2014), 1253-1268.

[21] Steen W.M. *Laser Material Processing*. Berlin: Springer. 2003.

[22] Seah M.P. and Spencer S.J. Repeatable intensity calibration of an X-ray photoelectron spectrometer. *Journal of Electron Spectroscopy and Related Phenomena* **151**(3) (2006), 178-181.

[23] Vasudevan R., Kennedy A.J., Merritt M., Crocker F.H. and Baney R.H. Microscale patterned surfaces reduce bacterial fouling-microscopic and theoretical analysis. *Colloids and Surfaces B: Biointerfaces* **117** (2014), 225-232.

[24] Valle J., Burgui S., Langheinrich D., Gil C., Solano C., Toledo-Arana A., Helbig R., Lasagni A. and Lasa I. Evaluation of surface microtopography engineered by direct laser interference for bacterial anti-biofouling. *Macromolecular Bioscience* **15**(8) (2015), 1060-1069.

[25] Fadeeva E., Truong V.K., Stiesch M., Chichkov B.N., Crawford R.J., Wang J. and Ivanova E.P. Bacterial retention on superhydrophobic titanium surfaces fabricated by femtosecond laser ablation. *Langmuir* **27**(6) (2011), 3012-3019.

[26] Korte F., Serbin J., Koch J., Egbert A., Fallnich C., Ostendorf A. and Chichkov B.N. Towards nanostructuring with femtosecond laser pulses. *Applied Physics A: Materials Science & Processing* **77** (2003), 229-235.

[27] Kurella A. and Dahotre N.B. Review paper: surface modification for bioimplants: the role of laser surface engineering. *Journal of Biomaterials Applications* **20**(1) (2005), 5-50.

[28] Snakenborg D., Klank H. and Kutter J.P. Microstructure fabrication with a CO_2 laser system. *Journal of Micromechanics and Microengineering* **14**(2) (2003), 182-189.

[29] Dyer P.E., Oldershaw G.A., and Sidhu J. CO_2 laser ablative etching of polyethylene terephthalate. *Applied Physics B: Lasers and Optics* **48**(6) (1989), 489-493.

[30] Lawrence J. and Li L. Modification of the wettability characteristics of polymethyl methacrylate (PMMA) by means of CO_2, Nd:YAG, excimer and high power diode laser radiation. *Materials Science & Engineering A. Structural Materials: Properties, Microstructure and Processing* **303**(1-2) (2001), 142-149.

[31] Waugh D.G. and Lawrence J. On the use of CO_2 laser induced surface patterns to modify the wettability of polymethyl methacrylate (PMMA). *Optics and Lasers in Engineering* **48**(6) (2010), 707-715.

[32] Lawrence J. and Li L. Wettability characteristics of polyethylene (PE) modified with CO_2, Nd:YAG, excimer and high power diode lasers. *Proceedings of the Institution of Mechanical Engineers Part B: Journal of Engineering Manufacture* **215**(12) (2001), 1735-1744.

[33] Hsu L.C., Fang J., Borca-Tasciuc D.A., Worobo R.W. and Moraru C.I. Effect of micro-and nanoscale topography on the adhesion of bacterial cells to solid surfaces. *Applied and Environmental Microbiology* **79**(8) (2013), 2703-2712.

[34] Hao L. and Lawrence J. *Laser Surface Treatment of Bio-Implant Materials*. Chichester: John Wiley & Sons. 2005.

[35] Lawrence J. Identification of the principal elements governing the wettability characteristics of ordinary Portland cement following high power diode laser surface treatment. *Materials Science & Engineering A. Structural Materials: Properties, Microstructure and Processing* **356**(1-2) (2003), 162-172.

[36] Hao L. and Lawrence J. CO_2 laser induced microstructural features in a magnesia partially stabilized zirconia bioceramic and the effects thereof on wettability characteristics. *Materials Science & Engineering A. Structural Materials: Properties, Microstructure and Processing* **364**(1-2) (2004), 171-181.

[37] Hao L. and Lawrence J. Effects of Nd:YAG laser treatment on the wettability characteristics of a zirconia-based bioceramic. *Optics and Lasers in Engineering* **44**(8) (2006), 803-814.

[38] Lee M., Zheng D., Sharma S.K., Troy P.J., Gyananath G. and Taylor G.T. Influence of surface properties on accumulation of conditioning films and marine bacteria on substrata exposed to oligotrophic waters. *Biofouling* **11**(1) (1997), 31-57.

[39] Chow T.S. Wetting of rough surfaces. *Journal of Physics: Condensed Matter* **10**(27) (1998), L445.

[40] Agathopoulos S. and Nikolopoulos P. Wettability and interfacial interactions in bioceramic-body-liquid systems. *Journal of Biomedical Materials Research* **29**(4) (1995), 421-429.

[41] Cassie A. and Baxter S. Wettability of porous surfaces. Transactions of the Faraday Society **40** (1944), 546-551.

[42] Eginton P.J. Gibson H. Holah J. Handley P.S. and Gilbert P. The influence of substratum properties on the attachment of bacterial cells. *Colloids and Surfaces B: Biointerfaces* **5**(3-4) (1995), 153-159.

[43] Armentano I., Arciola C.R., Fortunati E., Ferrari D., Mattioli S., Amoroso C.F., Rizzo J., Kenny J.M., Imbriani M. and Visai L. The interaction of bacteria with engineered nanostructured polymeric materials: A review. *Scientific World Journal* **2014** (2014), 410423.

[44] Taylor R.K., Pomianek M.E., Semmelhack M.F., Kraml C.M., Higgins D.A. and Bassler B.L. The major *Vibrio cholerae* autoinducer and its role in virulence factor production. *Nature* **450** (2007), 883-886.

[45] Liu Y., Yang S.F., Li Y., Xu H., Qin L. and Tay J.H. The influence of cell and substratum surface hydrophobicities on microbial attachment. *Journal of Biotechnology* **110**(3) (2004), 251-256.

[46] Pereni C.I. Zhao Q. Liu Y. and Abel E. Surface free energy effect on bacterial retention. *Colloids and Surfaces B: Biointerfaces* **48**(2) (2006), 143-147.

[47] Bakker D.P., Huijs F.M., de Vries J., Klijnstra J.W., Busscher H.J. and van der Mei H.C. Bacterial deposition to fluoridated and non-fluoridated polyurethane coatings with different elastic modulus and surface tension in a parallel plate and a stagnation point flow chamber. *Colloids and Surfaces B: Biointerfaces* **32**(2) (2003), 179-190.

[48] Liu Y. and Zhao Q. Influence of surface energy of modified surfaces on bacterial adhesion. *Biophysical Chemistry* **117**(1) (2005), 39-45.

[49] Taylor G.T., Zheng D., Lee M., Troy P.J., Gyananath G. and Sharma S.K. Influence of surface properties on accumulation of conditioning films and marine bacteria on substrata exposed to oligotrophic waters. *Biofouling* **11**(1) (1997), 31-57.

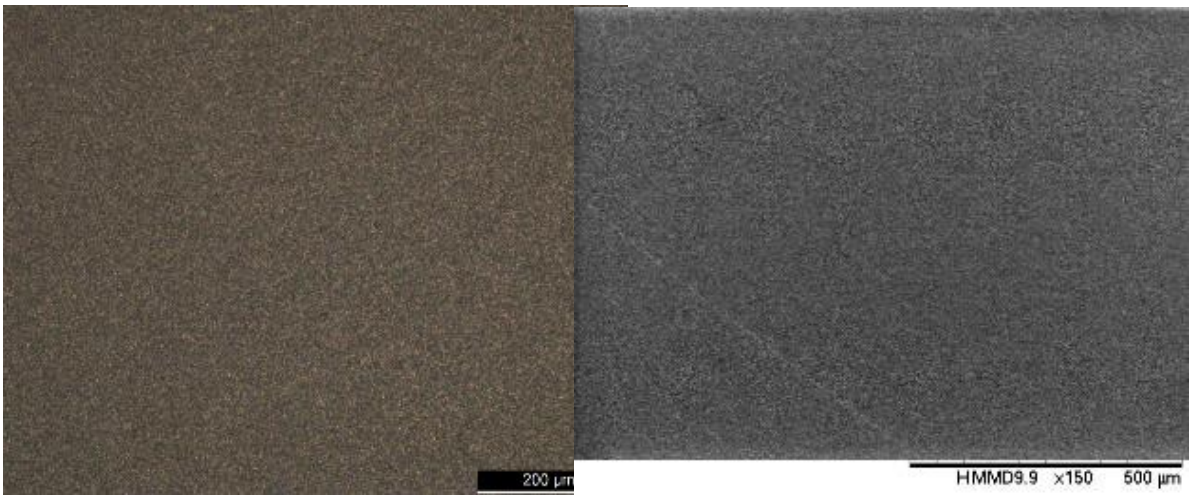
200 µm
HMMD9.9 x150 500 µm

(a) (b)

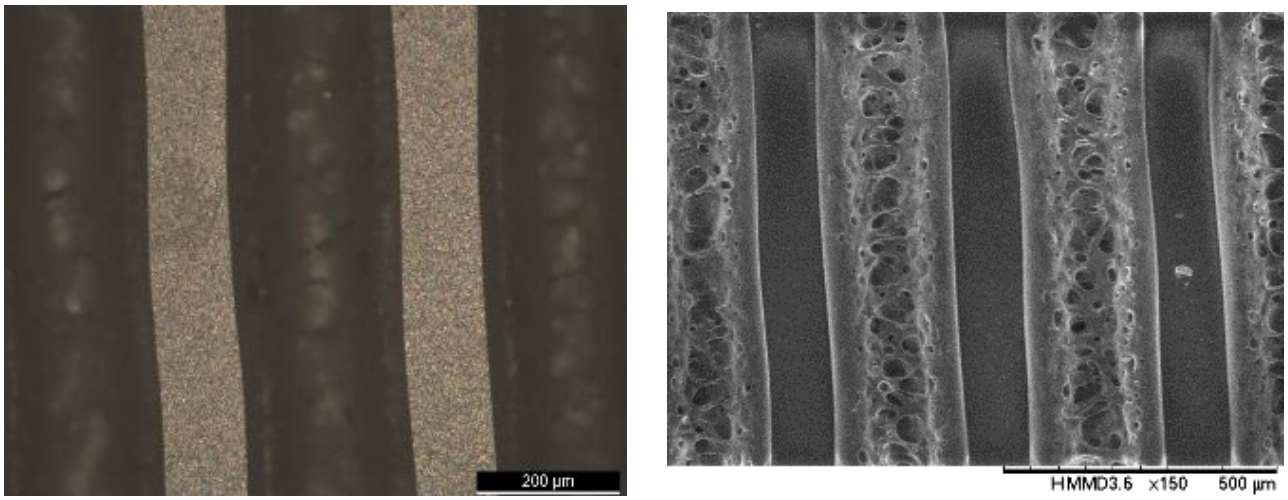
200 µm
HMMD3.6 x150 500 µm

(c) (d)

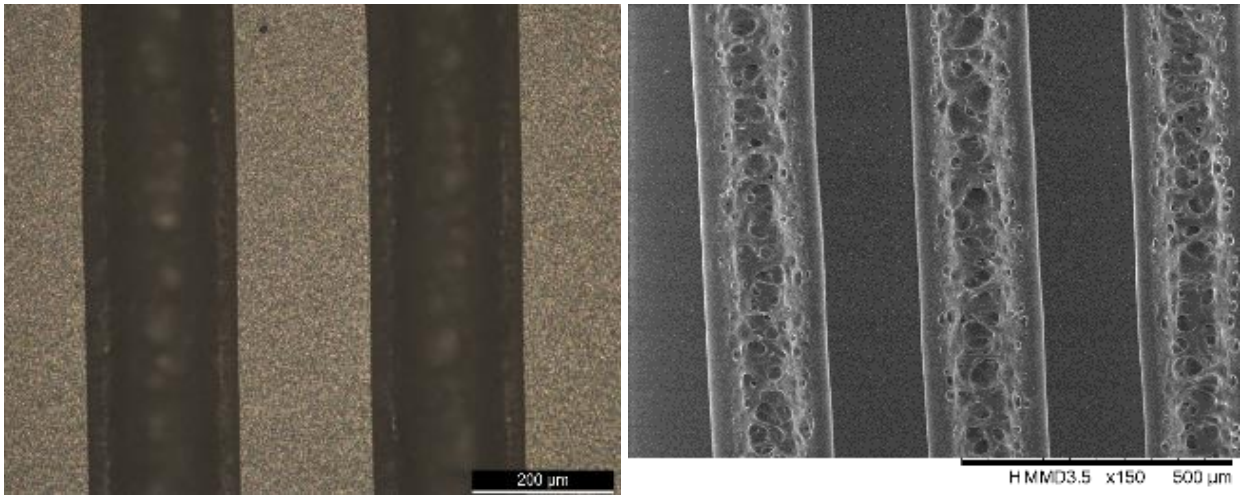
200 µm
HMMD3.5 x150 500 µm

(e) (f)

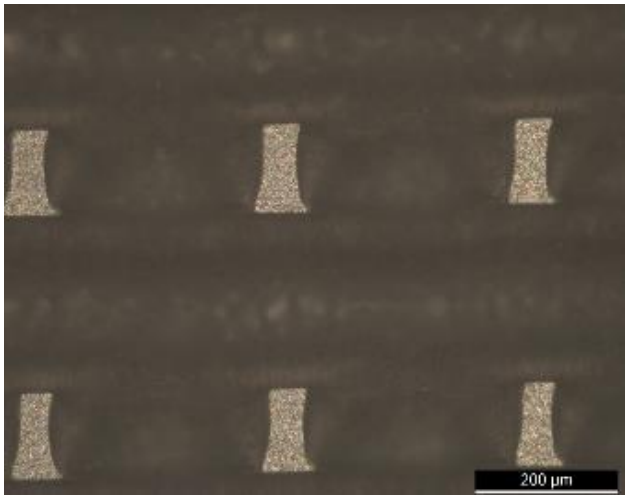

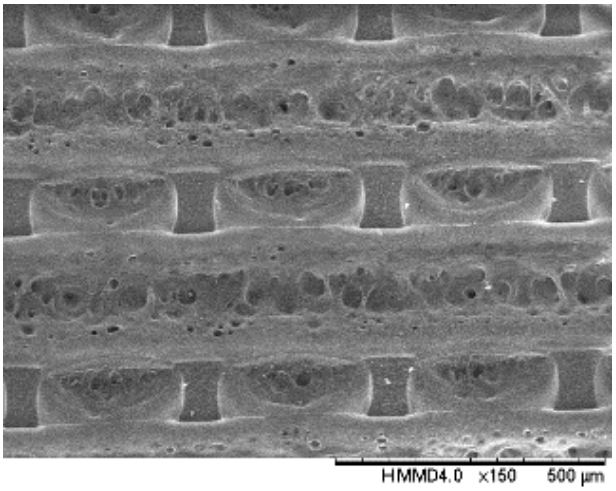

(g) (h)

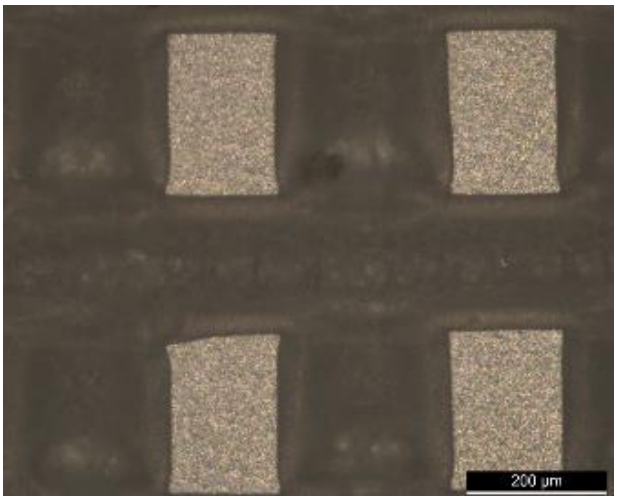

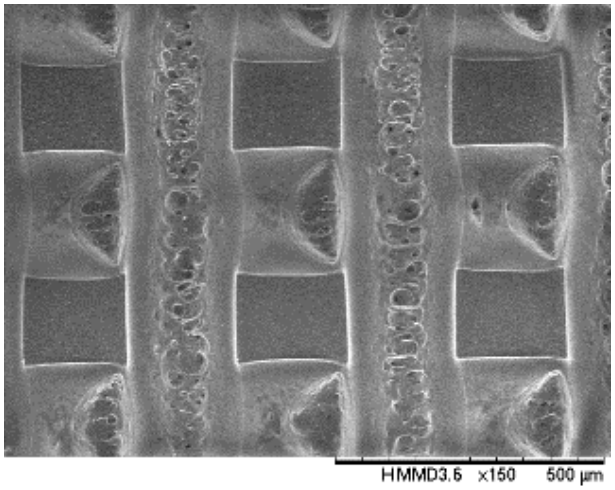

(i) (j)

FIGURE 1

Optical (left hand side) and SEM (right hand side) micrographs of as-received and CO_2 laser engineered PET films: (a and b) CO2SP_AR; (c and d) CO2SP_04; (e and f) CO2SP_05; (g and h) CO2HA_04; and (i and j) CO2HA_05.

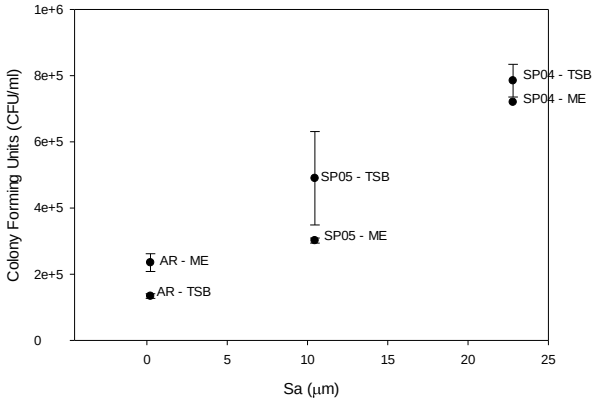

(a)

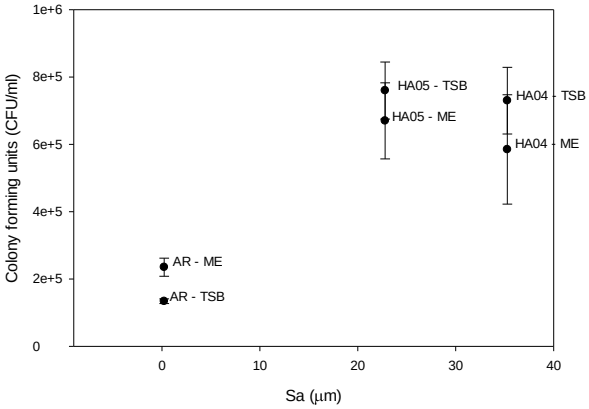

(b)

FIGURE 2

Graphs showing the comparison between surface roughness (S_a) of CO_2 laser engineered (a) the track patterns and (b) the hatch patterns with bacterial viable counts.

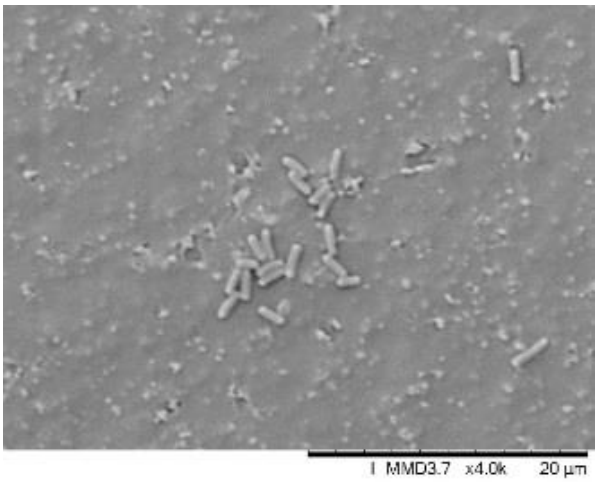

(a)

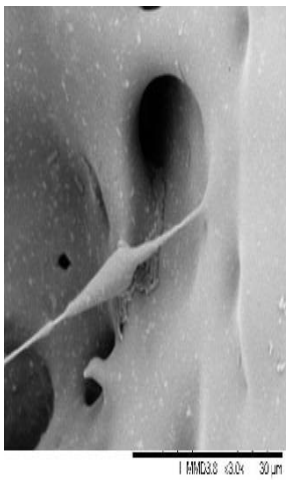

(b)

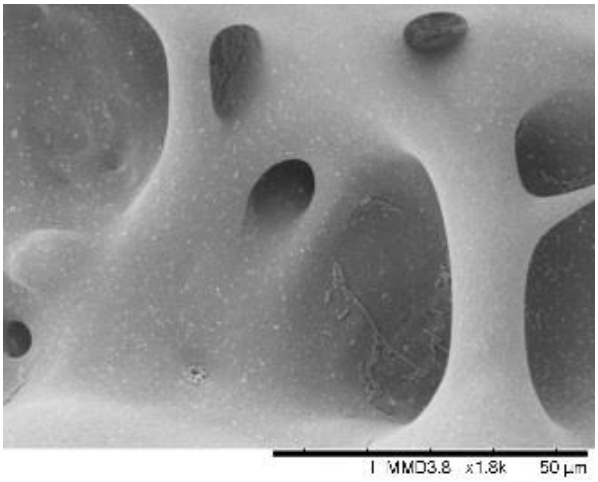

(c)

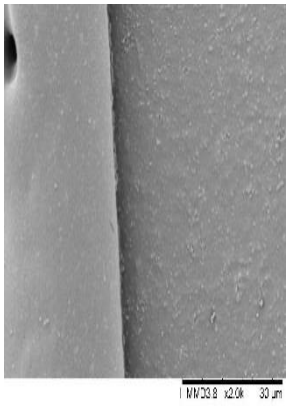

(d)

FIGURE 3

SEM micrographs of *E. coli* ATCC 25922 attachment to (a) the as-received PET sample (CO2SP_AR), and CO_2 laser engineered PET samples (b) CO2HA_05, (c) CO2SP_05 and (d) CO2SP_04.

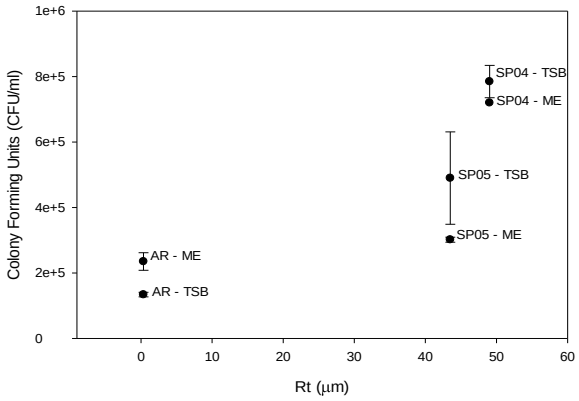

(a)

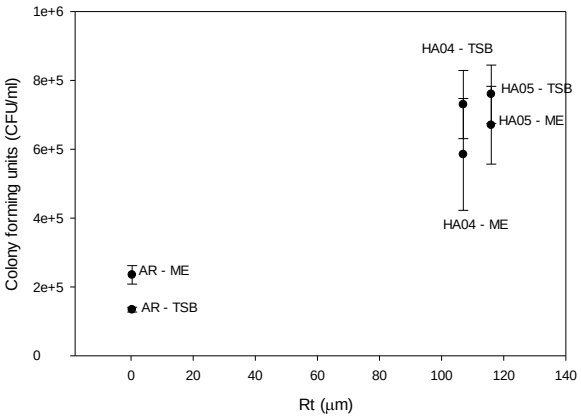

(b)

FIGURE 4

Graphs showing the comparison between vertical distance from the highest peak to the lowest valley (R_t) of CO_2 laser engineered (a) the track patterns and (b) the hatch patterns with bacterial viable counts.

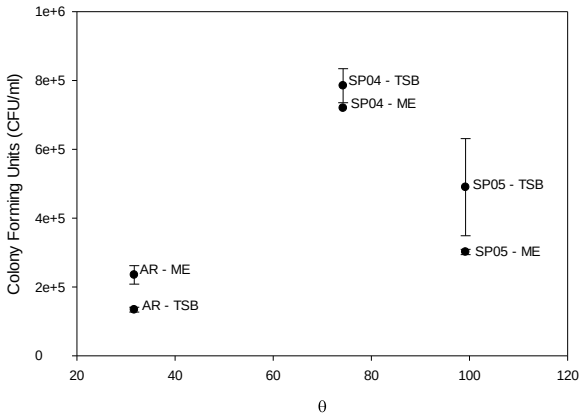

(a)

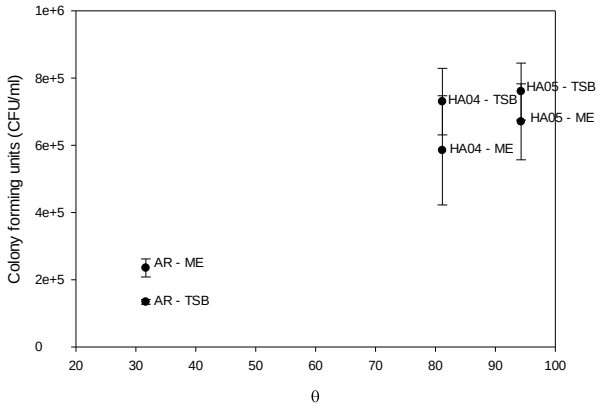

(b)

FIGURE 5

Graphs showing the comparison between contact angle measurements of CO_2 laser engineered (a) track patterns and (b) hatch patterns with bacterial viable counts.

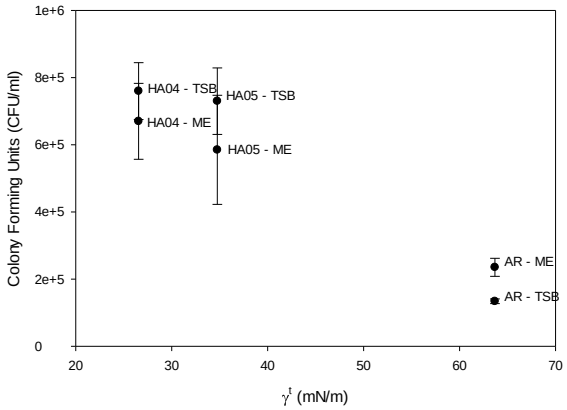

(a)

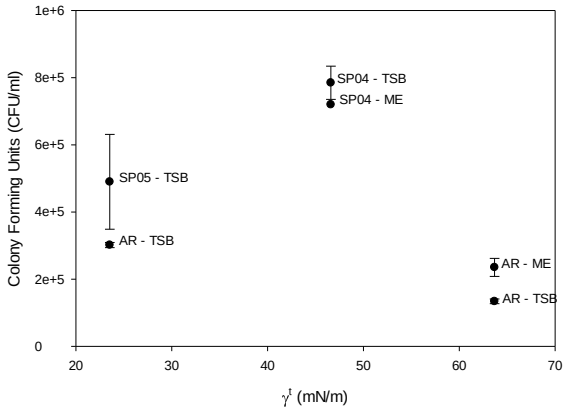

(b)

FIGURE 6

Graphs showing the comparison of total free surface energy of CO_2 laser engineered (a) the track patterns and (b) the hatch patterns with bacterial viable counts.

TABLE 1

Surface parameter data for each sample.

Sample Pattern	$\boldsymbol{R_a}$ **(µm)**	$\boldsymbol{S_a}$ **(µm)**	$\boldsymbol{R_t}$ **(µm)**	$\boldsymbol{R_{sk}}$
CO2_AR	0.06 ±0.01	0.22 ±0.13	0.36 ±0.04	-0.09 ±0.24
CO2SP_04	8.58 ±0.91	22.8 ±4.43	49.03 ±8.43	0.45 ±0.41
CO2SP_05	6.22 ±0.79	10.47 ±0.12	43.50 ±5.05	0.06 ±0.26
CO2HA_04	16.13 ±1.33	35.23 ±3.12	107 ±2.65	-1.21 ±0.47
CO2HA_05	13.07 ±0.81	22.8 ±0.92	116 ±4.36	-0.98 ±0.77

TABLE 2

Surface compositions of the as-received and CO_2 laser-treated PET samples as determined by XPS.

Element and Photoelectron Line	**Surface Composition (at.%)**				
	CO2_AR	CO2SP_04	CO2SP_05	CO2HA_04	CO2HA_05
Na 1s	0.3				
O 1s	24.6	26.6	26.2	26.0	26.1
N 1s	2.2	0.7	0.4	1.1	0.6
Ca 2p	0.3				
C 1s	71.7	72.5	73.0	71.7	72.6
S 2p	0.2				
P 2p	0.1				
Mg 2s	0.7	0.2	0.3	0.4	0.4
Si 2s/2p	0.03		0.1	0.7	0.2
F 1s					0.2

TABLE 3

Contact angle measurements formed by water droplets on the as-received and CO_2 laser engineered PET sample surfaces with corresponding surface energy values (PC denotes samples preconditioned with meat exudate).

Sample	θ (°)	γ^t (mN/m)	θ (°) (PC)	γ^t (mN/m) (PC)
AR	77.73 ±2.23	36.51 ±0.42	31.66 ±3.41	63.68 ±0.91
CO2SP_04	137.41 ±2.30	4.25 ±2.29	74.25 ±6.02	46.60 ±2.83
CO2SP_05	143.20 ±2.85	2.52 ±0.71	99.20 ±2.99	23.53 ±1.23
CO2HA_04	114.23 ±4.42	15.28 ±0.91	81.16 ±3.52	34.75 ±0.35
CO2HA_05	116.19 ±5.48	17.58 .64	94.29 ±5.63	26.55±0.42